Mon. Not. R. Astron. Soc. **334,** 77–86 (2002)

Orbital migrations in planetesimal discs: *N*-body simulations and the resonant dynamical friction

R. G. Cionco[1]★† and A. Brunini[1,2]‡

[1]*Facultad de Ciencias Astronómicas y Geofísicas. Universidad Nacional de La Plata. Paseo del Bosque s/n (1900) La Plata, Argentina*
[2]*Instituto de Astrofísica de La Plata, IALP, CONICET*

Accepted 2002 March 6. Received 2002 February 20; in original form 2001 September 4

ABSTRACT

We have performed *N*-body numerical simulations of the exchange of angular momentum between a massive planet and a 3D Keplerian disc of planetesimals. Our interest is directed at the study of the classical analytical expressions of the lineal theory of density waves, as representative of the dynamical friction in discs 'dominated by the planet' and the orbital migration of the planets with regard to this effect. By means of a numerical integration of the equations of motion, we have carried out a set of numerical experiments with a large number of particles ($N \geq 10\,000$), and planets with the mass of Jupiter, Saturn and one core mass of the giant planets in the Solar system ($M_c = 10\,M_\oplus$). The torque, measured in a phase in which a 'steady forcing' is clearly measurable, yields inward migration in a minimum-mass solar disc ($\Sigma \sim 10\,g\,cm^{-2}$), with a characteristic drift time of $\sim$ a few 10^6 yr. The planets predate the disc, but the orbital decay rate is not sufficient to allow accretion in a time-scale relevant to the formation of giant planets. We found reductions of the measured torque on the planet, with respect to the linear theory, by a factor of 0.38 for M_c, 0.04 for Saturn and 0.01 for Jupiter, due to the increase in the perturbation on the disc. The behaviour of planets whose mass is larger than M_c is similar to the one of type II migrators in gaseous discs. Our results suggest that, in a minimum mass, solar planetesimals disc, type I migrations occur for masses smaller than M_c, whereas for this mass value it could be a transition zone between the two types of migration.

Key words: stellar dynamics – celestial mechanics – planets and satellites: general – Solar system: formation – planetary systems.

1 INTRODUCTION

A plausible scenario for the formation of planetary systems assumes the coeval of a gaseous nebular phase with a solid one. It is widely accepted that, at least in our Solar system, the giant planets do form in a gas-rich environment, where they grow through a collisional process between planetesimals (Lissauer 1993). The presence of gas affects the dynamics of small planetesimals in the form of drag. When they reach a radius of $\sim O(10^3)$ km, a process known as the 'drag crisis' starts (Landau & Lifshitz 1959) with the development of a turbulent wake. In such circumstances, the gravitation begin to be relevant (Takeda et al. 1985) and a more appropriate treatment of the problem must be made (i.e. by the inclusion of tidal forces).

A planetesimal which departs sufficiently from the initial distribution of mass starts an accelerated growth (the 'runaway growth'), due to the fact that the dynamical friction with the rest of its environment reduces its relative velocity, thus enhancing its gravitational cross-section. The concept of dynamical friction was first introduced by Chandrasekhar (1942) in the context of stellar dynamics, to account for the process by which a massive body reaches the equipartition of energy with the background through gravitational interaction. This formulation assumes the massive body moving through an infinite background, so its application to discs in general and protoplanetary discs in particular is highly doubtful, e.g. in a protoplanetary disc the 'friction' comes mainly from the shear and not necessarily from the dispersion of velocities, as is the case in the Chandrasekhar dynamical friction formulation. On the other hand, the two-body approximation is not valid because of the fact that the tidal action of the central star during close encounters is not negligible (Ida 1990).

The formulation of dynamical friction for particulate discs comes from the stellar dynamics, and it is shown by Lynden-Bell & Kalnajs (1972, hereafter LBK). In that paper, the authors show that

★E-mail: cionco@pluton.fcaglp.unlp.edu.ar
†Fellow of CONICET.
‡Member of CONICET.

a uniformly rotating potential exerts torque on the disc only in resonant locations (we call this kind of transfer 'resonant dynamical friction' or 'resonant torque'). Therefore, at the last stages of planetary accretion, when the short-range interactions cease to be important, the planets must be gravitationally coupled to the protoplanetary disc.

For 2D cold gaseous discs ($c/\Omega r \ll 1$; c is the speed of sound and Ω is the orbital frequency at distance r), Goldreich & Tremaine (1979; hereafter GT79) have developed a theory for resonant torque driven by density waves, showing that in this particular case the formulation is equivalent to the resonant dynamical friction. In another pioneer paper, Goldreich & Tremaine (1980; hereafter GT80) estimated for the first time the speed of migration of a planet embedded in a protoplanetary nebula of low mass. They gave an estimation of the magnitude of the speed of migration without analysing its direction. GT80's result is conclusive: the core of a giant planet can decay to the central star in a time-scale shorter that the time for its complete accretion. This result encouraged a number of investigations about the interaction of a planet with the gaseous disc, the most conspicuous nebular component. With regard to the planetary migration and the magnitude of the resonant torque, most researches have focused their attention to the direction of the migration, the reduction of the effect due to 3D geometry and the opening of gaps in the region of the disc surrounding the planet. Ward (1986) has shown that, even in discs with very different profiles, the migration is, in general, inwards. Actually, the net torque is ruled by intrinsic asymmetries rather than detailed flow properties (e.g. Ward 1997). Ward (1988) and Artymowicz (1993) have studied the effect of the thickness of an isothermal and stratified disc (as a superposition on z of infinitesimal discs). They found that the torque is reduced by ~ 50 per cent with regards to the transfer predicted by the 2D theory, due to the smoothness of the gravity of the planet in the 3D geometry.

The well known regimes of migration has been analysed in a unified model by Ward (1997). He has shown how a growing planet evolves from a linear regime (type I) to a non-linear one (type II), with gaps opening with the increasing of the planet mass. In this last stage, as non-linear effects become important, the torque on the planet is reduced and the orbital evolution finally follows a constant rate, independently of the mass. The amount of this reduction can be of orders of magnitude.

Recent numerical simulations of the gaseous flux around a protoplanet, for an isothermal (in the z-component) 3D disc (Myoshi et al. 1999; Tanaka, Takeuchi & Ward 2000) would confirm the theoretical estimations of the 2D theory, in the case where the tidal radius of the planet is less than the scaleheight of the disc. That is, in 3D, a type I migrator would reduce its speed of migration by a factor of 0.5 or even less. For larger perturbers, simulations by Kley, D'Angelo & Henning (2001) have shown that both 2D and 3D discs present the same behaviour. These works have shown how important the non-linearity the 3D effect is, but as the planet becomes a large perturber both geometries yield the same result. This can be understood easily in terms of the growth of the tidal radius of the perturber, which in this case, exceed the high scale of the disc.

The planet–planetesimal disc interaction has been extensively studied by means of numerical simulations. However, at present there are no N-body simulations designed to study orbital migrations in planetesimal discs from a resonant perspective. Fernández & Ip (1984) have shown that a system of protoplanets embedded in a planetesimal disc can experience strong orbital migrations by the exchange of angular momentum with the surrounding planetesimals during close encounters. However, the attention of most papers was focused at the end of the runaway phase, with special emphasis on the structure of the disc in the neighbourhood of the protoplanet (Ida & Makino 1992, 1993). In particular, Ida & Makino (1993) have shown that even for a small (non-migrating) protoplanet the interaction evolves from a 'planet–planetesimal–planetesimal' interaction to a 'planet-dominated stage' (planet–planetesimal interaction), in which the planet becomes a strong disc perturber, scattering the disc and slowing down the runaway growth. We show in this work that for larger perturbers, the tidal effects are reduced due to gap opening (non-linear effects), producing a strong scattering of the planetesimals, with the subsequent ejection of particles of the system. Ward & Hahn (1995) and Tanaka & Ida (1999) have studied how a migrating protoplanet (due solely to the interaction with the gaseous component of the disc) affects the accretion process at the end of the runaway stage. Murray et al. (1998) suggested that a massive disc of planetesimals can induce inwards migrations of protoplanets.

The decay of galactic satellites as a result of the action of resonant dynamical friction has been extensively studied. We have found in these kind of studies, the works sharing the major methodological similitude with our own work (Wahde, Donner & Sundelius 1996, and references therein). The effect of the dispersion of velocities and of the self gravitation have been studied by Wahde et al. (1996). Their results were conclusive in the sense that this effect have a negligible effect on the observed dynamical friction. It is worth noting here that the extrapolation of these results to the case of protoplanetary discs is not evident. In addition, in these simulations the satellite does not interact only with the disc but also with other galactic structures.

In this work, we have simulated the dynamical interaction between a massive planet and a non-self-gravitating Keplerian 3D disc with a large number of planetesimals. The planet can migrate freely within the disc and the disc can evolve without limits. N-body simulations with large number of particles enable us to study the problem in a resonant perspective, together with other interactions as scattering, ejection, encounters and accretion. We focus our attention to the possible migrations in a minimum mass solar nebula model, and the magnitude of the torque on the planet, in order to investigate the behaviour of the classical formulation of the 2D resonant torque (linear theory of density waves in 2D). These migrations are relevant not only in their cosmogonical implications, but also in the light of the recently discovered extrasolar planets close to the central star (e.g. see the Extrasolar Planets Encyclopedia[1]), and as a way to extend the phase of runaway growth.

In Section 2 we will describe the numerical model and the main results of our simulations. In Section 3 we will estimate the torque from the orbital decay. In Section 4 we will describe the effect of the planets on the disc. Section 5 is devoted to the resonant torque formulae. Sections 6 and 7 describe how we have applied these formulae. The last section is devoted to the conclusions.

2 NUMERICAL SIMULATIONS

Our model is composed of a planet of mass M and a number of planetesimals, each one of mass m', orbiting around the Sun. The self-interaction between the planetesimals was not considered.

[1] http://www.obspm.fr/encycl/encycl.html

This assumption is supported by the results of Ida & Makino (1993). They have shown that the mutual interaction between planetesimals is weaker than the effect due to the scattering by the protoplanet in the case $M/m' > 10^2$. In all our simulations we have $M/m' \gg 10^2$. The conclusions of Wahde et al. (1996) also support this model assumption. The equations of motion were integrated by means of a leap-frog simplectic integrator based in the one of Wisdom & Holman (1992). Close encounters with the planet are treated with the strategy of Chambers (1999), so our integrator is fully simplectic. The code allows accretion. Those planetesimals falling on to the Sun or acquiring hyperbolic orbits are eliminated from the integration. The simulations were performed for three different kinds of planets: Jupiter (M_J), Saturn (M_S) and a 'one core mass' planet ($M_c = 10\,M_\oplus$) at 5 au. The initial orbital eccentricities where of 0.05, compatible with a near circular planetary orbit. The discs were constructed with constant surface density of the order of $\sim 10\,g\,cm^2$, consistent with a model of minimum mass solar nebula ($0.01\,M_\odot$). The boundaries of the disc were $[0.4, 2.2]a$, a being the semi-major axis of the planet. This limits guarantee the inclusion of the most distant resonances involved in the theoretical determination of the resonant torque to the second order in the eccentricity (GT80).

In all our simulations, the initial orbital eccentricities and inclinations of the particles were generated at random with uniform probability distribution in the interval $(0–5) \times 10^{-3}$.

With the objective of checking the sensitivity of the results with respect to some of the parameters of our model, we have performed some previous simulations. For us, the main result of the simulations is the variation of the planetary semi-major axis, because we expect to determine the migration speed and the torque on the planet from it.

In the test runs we have varied the number of planetesimals, the mass and limits of the simulated disc, the index k in the radial distribution of planetesimals and the initial orbital inclinations and eccentricities of the planetesimals.

At constant disc mass, the number of particles is of great importance. The noise introduced by the 'granularity' (defined by the relation M/m') produces jumps into the temporal evolution of the semi-major axis of the planet. Regarding the variation of the semi-major axis, it is possible to establish two main stages, which were observed in all the simulations, as follows.

(i) The transitory phase: initial oscillations and jumps of different magnitude, producing stochastic migrations.

(ii) The stationary phase: the stage of an almost constant rate of change of the planetary semi-major axis. The jumps and oscillations are of small amplitude.

We expect to determine the migration and the torque on the planet in this last stage. The duration of the stationary phase was notably less than 10^5 yr for all the runs. After this period, it is very difficult (sometimes impossible) to obtain the dynamical friction force, because of rapid variations in semi-major axis and larger discrepancies between the runs for each case.

The jumps are reduced with the increase in the number of particles, but they never completely disappear. After many checks, we have utilized 1×10^4 planetesimals for the cases of Jupiter and Saturn, and 2×10^4 for M_c. On average, we have obtained similar results with an even larger number of particles, but with an important additional computational cost.

The way the perturber is introduced might be of great relevance for phase (i). As the initial conditions for the planetesimals were generated as if the planet was not present, we have made runs introducing the planet in different ways. Unfortunately, it was impossible to eliminate the initial jumps (as is also mentioned by Wahde et al. 1996). In the case of Jupiter, phase (i) was of $\sim 1 \times 10^4$ yr, and for the other ones it was $\sim 2 \times 10^4$ yr.

Table 1. Parameters of the simulations. The semi-major axis of the planet is a, Σ is the 'exact' density value.

	M_{disc} [M_J]	a [au]	Σ [g cm^{-2}]	N_{Part}	m' [$M_\oplus$]
Jupiter	0.5	5	12	10×10^3	0.017
Saturn	0.5	5	12	10×10^3	0.017
Core	0.5	5	12	20×10^3	0.008

We have also experimented with different radial distributions of planetesimals of the form r^k. The index k does not introduce appreciable effects. Therefore it is possible, in principle, to recreate different densities. We have estimated the simulated density as:

$$\Sigma(r) = \frac{m' No (r/1UA)^k}{2\pi r \Delta r} = \Sigma_o (r/1UA)^{k-1}, \quad (1)$$

where m' is the planetesimal mass and No is certain number of particles distributed at the distance r in a ring of width $r - \Delta r/2 < r < r + \Delta r/2$. As the discs were generated as flattened systems, and as the results will be compared with the bidimensional theory, we have taken the 2D density as a reference. In Table 1 we show the 'exact' value of the density for each simulation (we have used $k = 1$), joint with other relevant parameters of the simulations.

For each of the three cases, we have carried out four runs with different seed numbers, which were necessary to generate the initial conditions of the planetesimals. The results for each case is the average over the four runs. With this procedure, we hope to smooth out the stochastic effects, which are always present in N-body simulations. The step size of integration was $\leq 10^{-2}$ of the smallest orbital period in each simulation.

2.1 General results

As it is shown in Fig. 1 for one of the runs of Jupiter, the planets develop a trailing spiral pattern, evidentiating the resonant structure of the disc (obviously this pattern is less evident for the other cases). The disc is perturbed in the neighbourhoods of the Lindblad and co-rotation resonances (see Section 5.1). After the initial stage, the density of the disc acquires a characteristic profile, as is shown in Fig. 2 for Jupiter. This figure displays the number of particles at $t = 0$ and $t = 2 \times 10^4$ yr. The initial location of the resonances in the disc are also marked. It can be appreciated clearly how after $t = 2 \times 10^4$ yr the disc is excited near the resonances. The shift is due to the planetary migration. A deep gap appears in the zone of overlapping of resonances. The gap is very similar for Jupiter and Saturn simulations, and it is shallower in the core mass planet case. In this last case the planet ejected almost 50 per cent of the particles.

One central point of our simulations is when the torque on the planet should be measured. We should seek a time-interval in which the nearly constant variations of the semi-major axis are not strongly affected by relaxation or saturation of resonances, (always present in N-body simulations), in order to perform the comparison against the theory. Therefore, the time-interval used to measure the planetary migration rate in each case was determined in the way proposed by Wahde et al. (1996).

The rate of migration for each case (the 'observed migration rate') was obtained by means of a least-squares fit over the

averaged semi-major axis of the four runs, performed during a time-interval where the conditions prescribed above were satisfied in all of them. We have carried out several tests for different time-intervals, and we found a maximum variation in the results by a factor of less than 2. Therefore, this parameter of migration must be considered like an extrapolation, and are important if their rate remains constant. This kind of extrapolation is used, for example, in Nelson et al. (2000), where the decay time is computed in a time-interval shorter than the simulated one.

We have also fitted the decay of the semi-major axes for each particular run, in order to have an idea of the dispersion of the results.

In what follows we will describe the particular results of each one of the three cases.

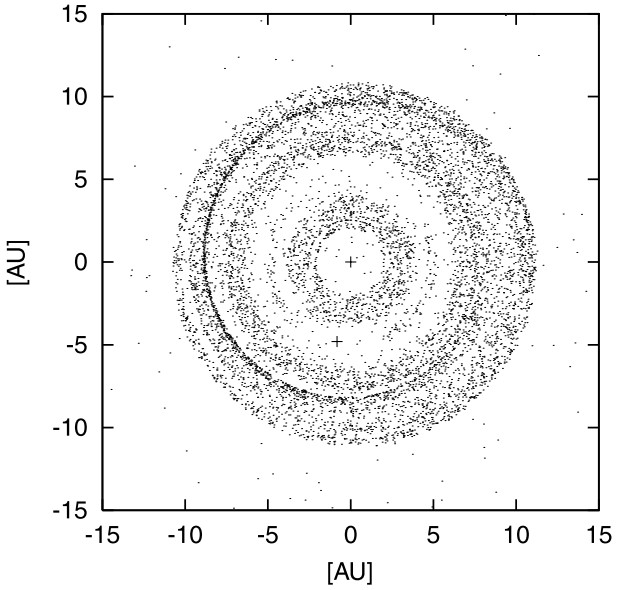

Figure 1. Trailing spiral pattern developed in one of the runs of Jupiter after 10^4 yr. The plus signs indicate the locations of the Sun and Jupiter.

2.2 Jupiter

Initially placed at 5 au, we extended the disc in the region [2–11] au, distributing 0.5 Jupiter mass through 10^4 particles. Therefore, the mass of each particle is $0.0167\,M_\oplus$ ($M/m' \simeq 19\,000$). Following the prescription quoted above, we have measured the decay rate in the time-interval $(10–35)\times10^5$ yr. The results, averaging over the four runs with different random numbers, are:

(i) observed migration rate $\langle\dot{a}\rangle = -0.94\times10^{-6}$ au yr^{-1};
(ii) characteristic drift time $\tau = a/\langle\dot{a}\rangle = 5.32\times10^6$ yr.

The migration rates fitted to each individual run presented maximum variations of 0.4–1.5 times the mean value. Fig. 3 shows the averaged change in the semi-major axis for Jupiter, normalized to the initial one.

2.3 Saturn

Saturn was initially placed at 5 au. The disc parameters are the same as in the Jupiter case. The granularity factor is $M/m' \simeq 5500$. The average results for the four runs were computed within the interval $(20–80)\times10^3$ yr, giving:

(i) observed migration rate $\langle\dot{a}\rangle = -1.07\times10^{-6}$ au yr^{-1};
(ii) characteristic drift time $\tau = a/\langle\dot{a}\rangle = 4.67\times10^6$ yr.

The variations were, in this case, of 0.6–2.4. Fig. 4 shows the averaged change in the semi-major axis for Saturn, normalized to the initial one.

2.4 One core mass

The planet was initially placed at 5 au, and the planetesimals were distributed in the region [2–11] au. The total disc mass was the same as in the case of Jupiter in order to obtain the same density. However, in order to increase the granularity, the number of particles was set at 2×10^4. In this way the mass of each planetesimal is $0.0083\,M_\oplus$ ($M/m' \simeq 1200$). The main results (measured within the interval $(20–80)\times10^3$ yr are:

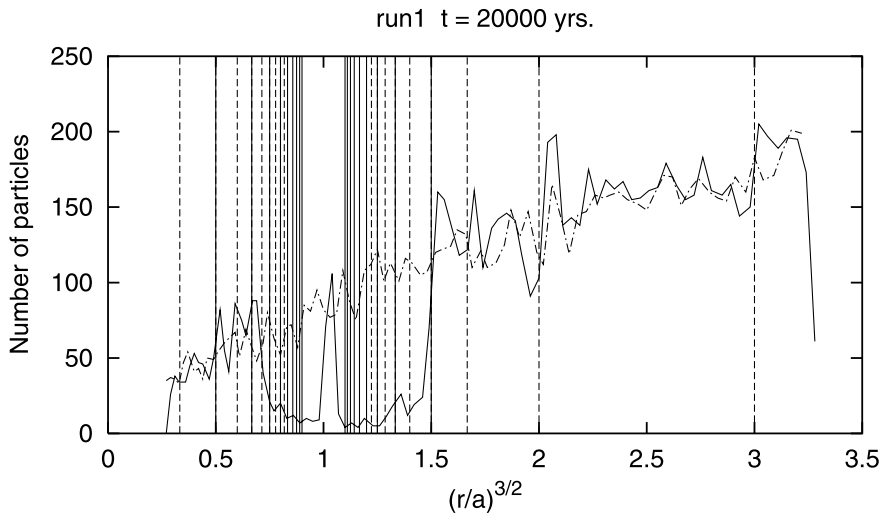

Figure 2. Number of particles at $t = 0$ (dash-dotted line) and $t = 2\times10^4$ yr (solid line) for one of the Jupiter runs. The initial location of the resonances in the disc are also marked with vertical lines (solid lines: circular resonances, dashed lines: eccentric resonances).

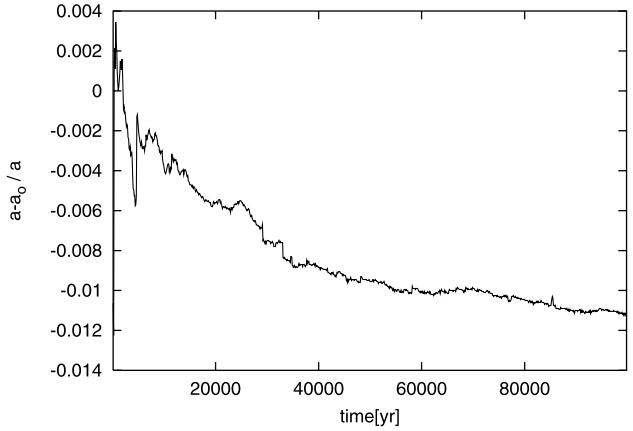

Figure 3. Temporal evolution of the semi-major axis for the case of a planet with Jupiter mass initially at 5 au, averaged over four runs.

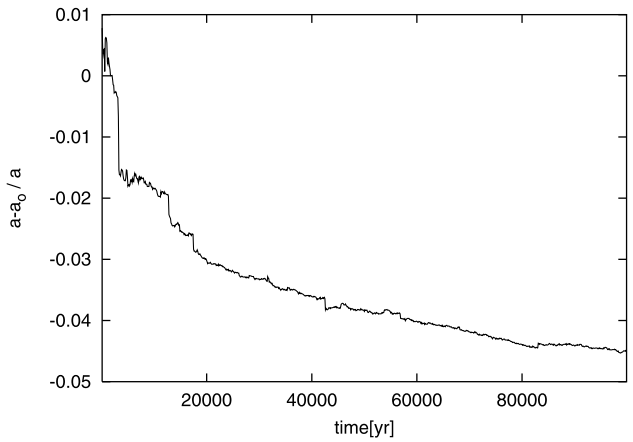

Figure 4. Temporal evolution of the semi-major axis for the case of a planet with Saturn mass initially at 5 au, averaged over four runs.

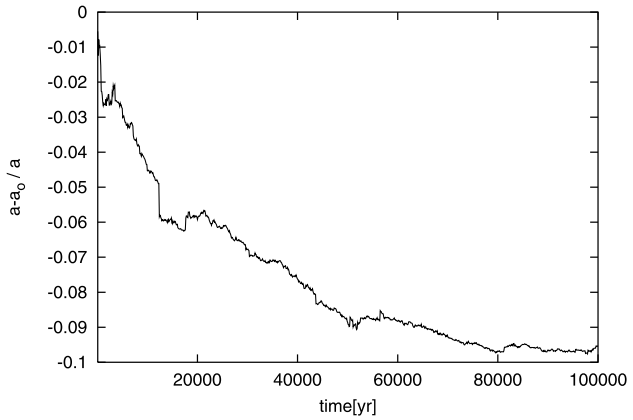

Figure 5. Temporal evolution of the semi-major axis for the case of a planet with a $10\,M_\oplus$ mass initially at 5 au, averaged over four runs.

(i) observed migration rate $\langle \dot{a} \rangle = -3.22 \times 10^{-6}$ au yr^{-1};
(ii) characteristic drift time $\tau = a/\langle \dot{a} \rangle = 1.55 \times 10^{6}$ yr.

The maximum variations were found to be of 0.4–1.8. Fig. 5 shows the averaged change in the semi-major axis for M_c, normalized to the initial one.

Table 2. Migration rate, characteristic drift time and torque on the planet, obtained from the simulations.

	da/dt [au yr^{-1}]	τ [yr]	Γ [$M_\odot$ au^2 yr^{-2}]
Jupiter	-0.94×10^{-6}	5.32×10^{6}	-1.31×10^{-9}
Saturn	-1.07×10^{-6}	4.67×10^{6}	-0.55×10^{-9}
Core	-3.22×10^{-6}	1.55×10^{6}	-0.14×10^{-9}

3 DETERMINATION OF THE TORQUE FROM THE ORBITAL MIGRATION

The reaction torque that the disc exerts on the planet can be estimated from the orbital decay and the rate of variation of the orbital angular momentum of the planet. From two-body dynamics, it is straightforward to relate the torque on the planet with its migration. The observed behaviour of the disc suggests that the variation of the z-component of the angular momentum almost introduces the totality of the torque. Therefore, it is valid to suppose that the planet experiences a net tangential perturber acceleration $A = \Gamma/aM$, where Γ is the torque exerted for the disc on the planet of mass M with semi-major axis a, and orbital frequency Ω. At first order in the eccentricity, we have

$$\Gamma = 0.5 a \Omega M \frac{\mathrm{d}a}{\mathrm{d}t}. \quad (2)$$

Therefore, by means of the equation (2) we obtain the 'observed' torque related to the observed migration rate, da/dt. Its values are shown in Table 2.

We have obtained almost identical results from the variations of the orbital angular momentum of the planet. This is due to the fact that the planetary eccentricities are always very small.

4 PREDATE ACTION, GAP FORMATION AND SCATTERING: THE DESTINY OF PLANETESIMALS

The planets predate the disc (Ward & Hahn 1995; Tanaka & Ida 1999) with an intensity proportional to the speed of migration. In Fig. 6 the predating action is shown for a particular run of M_c case planet. The orbital instabilities generated by the overlapping of resonances close to the planet open a gap, but as a result of the migration there are planetesimals entering the feeding zone, where the Tisserand parameter is less than 3 (Danby 1962). We have taken the width of the gap as the distance were the density of planetesimals drops abruptly with respect to the original density, and we find that its width is related to the Hills' radius of the planet by a factor of close to 7 in all the cases. In Table 3 the half-width of the gap and the Hills' radius of the planets are given. At difference with the predating action, the accretion is negligible in the time-span of the simulations (no accretion was detected for the Jupiter and Saturn cases, for M_c two planetesimals hit the planet, on average). This fact could be relevant for giant planet formation (Pollack et al. 1996). It suggests that even for a migrating $10\,M_\oplus$ protoplanet, it is difficult for a solid core to exceed this mass value in a planetesimal disc of minimum nebular mass. The effect of the gaseous component of the protoplanetary nebula could play an important role in this question.

The ejections are in general important, and, as it is shown in Fig. 6, they occur mainly in the gap zone. Jupiter and Saturn ejected almost 80 per cent of the initial particles in this zone. Even

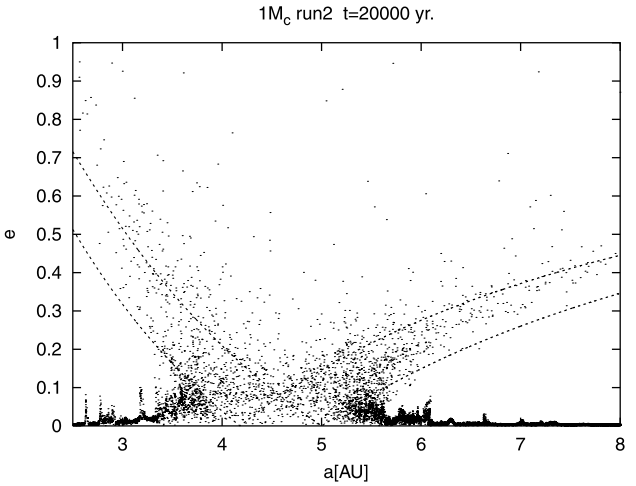

Figure 6. Snapshot at $t = 2 \times 10^4$ yr of the distribution of semi-major axes and eccentricities of the particles in the case of M_c. The scattered particles are distributed along the curves of constant values of the Jacoby integral. However, the predated action is evident, as particles are not swept up by the planet during the migration. At resonant locations, the orbital eccentricity of the particles is pumped up. The dashed lines represent the loci of the Tisserand parameter $T = 3$ at $t = 0$ and $t = 2 \times 10^4$ yr.

Table 3. Hill's radius and gap half-width in units of R_H.

	R_H [au]	gap width
Jupiter	0.35	3.7
Saturn	0.23	3.6
Core	0.11	3.4

M_c ejected approximately 50 per cent of the particles in the gap zone, therefore it must be considered a 'gap opener'.

Considering that the particles are ejected mainly in the coorbital region, the variation of the energy by the ejection of a mass $\Delta m'$ is $\Delta E_{m'} = G\mathrm{M}_\odot \Delta m'/2a$. As the total energy of the system is conserved, the variation in the energy of the planet is $\Delta E_M = -G\mathrm{M}_\odot M \Delta a/a^2$, and therefore

$$\Delta a = -0.5a\frac{\Delta m'}{Mp}. \tag{3}$$

This migration is consistent with a net torque (which can be obtained from equation 2):

$$\Gamma = -0.25L_0\frac{\mathrm{d}m'}{\mathrm{d}t}, \tag{4}$$

where L_0 is the specific angular momentum of the planet in the case of circular orbit and $\mathrm{d}m'/\mathrm{d}t$ is the rate of ejection of planetesimals. In Section 7, we will apply this equation to estimate the effect of the ejected particles.

5 THE RESONANT TORQUE

A perturber embedded in a particulate disc exert torques solely into resonant locations (LBK). The LBK formulation starts from the 'epicyclic description', and from a fluid approximation through a 'distribution function', which, for flattened systems, only depends on the energy and the angular momentum. The dynamics of the disc is described by means of action-angle variables which are associated to harmonic numbers l, m in the Fourier decomposition of the perturbation. The action of the perturber induces a spiral pattern of m arms. If the spiral pattern is trailing, the angular momentum is transferred from the inner disc to the outer one.

The main hypothesis of the LKB formulation is that the flux around the perturber must be stationary. This hypothesis is equivalent to introduce the planet smoothly. The angular momentum is transferred at resonant locations ($r = r_{es}$), where

$$\frac{l}{m}\kappa(r_{es}) + \Omega(r_{es}) - \Omega_{PS} = 0, \tag{5}$$

where κ is the epicyclic frequency, Ω is the circular frequency ('guide centre' of the epicyclic motion) and Ω_{PS} is the pattern speed of the lm component of the Fourier decomposition of the disturbing potential.

At the places where the wave pattern corotates with the circular frequency, there are 'corotation resonances' ($l = 0$), whereas we have 'Lindblad' resonances ($l = \pm 1$) where the natural frequency of the disc (κ) is equal to the frequency of the perturber, shifted by the Doppler effect (the perturbation finds the particle at the same position in the epicycle).

GT79 have demonstrated that in the limit $J1 \ll \kappa r^2$, where $J1$ is the radial action, the formulation LKB is equivalent to the formulation of external torques on gaseous discs. The above condition implies that $J1$ should be much less than the 'epicyclic momentum', or in other words, that the epicyclic approximation must be perfectly valid (which is equivalent to the condition $c/\Omega r \ll 1$ in the GT79 formulation).

The first application of the resonant theory to the planet–disc interaction is performed by GT80. They have considered a planet on eccentric orbit. The potential due to the planet, in the epicyclic approximation is $\Phi_p \propto \Phi_{lm}\cos[m(\theta - \Omega_{lm}t)]$, where $\Omega_{lm} = \Omega(a) + (l - m/m)\kappa(a)$ is the pattern speed of the perturbing potential (the l, m numbers are not exactly the same than in the LBK theory, and Φ_{lm} is the amplitude of the perturbing potential). The guide centre and the epicyclic frequency of the planet is evaluated in a, which differs from the Keplerian semi-major axis a_K by

$$a \simeq a_K(1 + 2e^2), \tag{6}$$

to the first order in the epicyclic amplitude. Following GT79 and GT80, the torque at Lindblad resonances is given by

$$T^L_{l,m} = -m\pi^2\Sigma\frac{\Psi^2_{l,m}}{D'} \tag{7}$$

where $D' = r(\mathrm{d}D/\mathrm{d}r)$, $D = \kappa^2 - m^2(\Omega - \Omega_{lm})^2$ and Ψ_{lm} is the lm component of the Fourier decomposition of the perturbing function. The torque at corotation resonances is

$$T^C_{l,m} = -m\frac{\pi^2}{2}\Phi^2_{l,m}\left(\frac{\mathrm{d}\Omega}{\mathrm{d}r}\right)^{-1}\ \frac{\mathrm{d}}{\mathrm{d}r}\left(\frac{\Sigma}{B}\right), \tag{8}$$

where $B = \Omega/4$ is one of the Oort constants. For the Lindblad torque the sign of D'/T is negative. In the outer disc, $D' < 0$, and conversely in the inner disc. Therefore, the outer disc gains angular momentum at expenses of the inner disc. For corotation torques, the first bracket is negative. The sign depends on the value of the second bracket (the vorticity gradient), which is equal to 0 for a disc with a Keplerian density profile. For a gaseous disc, the planet transfers angular momentum to the Lindblad resonances, and it is transported away by a density wave. In particulate discs without self-gravity like ours, no density waves should be excited: the planet transfers angular momentum to the Lindblad resonances and it is absorbed by the particles. At corotation there is no net transport of the angular momentum deposited by the planet.

5.1 Resonances

As was already mentioned, the epicyclic description implies the existence of two basics resonances.

Following equation (6), as in our case $e \ll 1$, we will consider all the resonant frequencies referred to the planet, evaluated into the Keplerian semi-major axis. Lindblad resonances occur if

$$m[\Omega(r_{\rm es}) - \Omega_{lm}] = -\epsilon\kappa(r_{\rm es}), \quad m \geq 1, \tag{9}$$

where $\epsilon = -\mathrm{sgn}\,(D') = 1$ for the outer disc and -1 for the inner disc. For the potentials $l = m$ we have *circular* resonances, 'inner' (-1) and 'outer' $(+1)$, which are the only ones excited by a circular perturber. In a Keplerian disc ($\kappa = \Omega$),

$$\frac{\Omega(a)}{\Omega(r_{\rm es})} = (r_{\rm es}/a)^{3/2} = \frac{m+\epsilon}{m}, \tag{10}$$

which is equivalent to the usual relation of mean motion commensurability

$$\frac{\Omega(a)}{\Omega(r_{\rm es})} = \left(\frac{j+1}{j}\right)^{\epsilon}, \quad j \geq 1. \tag{11}$$

As the GT80 formulation includes the indirect part of the perturbing function for $m = 1$, both resonances are equal if $m = j + 1$. For the potentials with $l = m + \epsilon$ we have *eccentric* resonances (inner and outer);

$$(r_{\rm es}/a)^{3/2} = \left(\frac{1-m}{1+m}\right)^{\epsilon} \tag{12}$$

for each pair of resonances (inner–outer) there is also a couple of resonances which are 'coorbital' with the perturber ($r_{\rm es} = a$).

The corotation resonances occur at locations where

$$\Omega(r_{\rm es}) = \Omega_l m. \tag{13}$$

For $l = m$ they are coorbitals with the perturber. In the case $l - m = \epsilon$, the corotation resonances coincide with the circular ones, because the pattern speed of the potential contains the epicyclic motion around the guiding centre.

At $r = a$ the resonances have an accumulation point (see Fig. 2). At certain m, where resonances begin to overlap, all the preceding expressions are no longer valid. In what follows we will call α to $r_{\rm es}/a$.

6 APPLICATION OF THE RESONANT TORQUE FORMULATION

One of our main scopes will be to compare the torque observed in our numerical simulations with the one obtained with the 2D linear theory of density waves.

For a particulate disc without a density gradient, the only source of asymmetry in the torque comes from the perturbing function and from the radial dependency of the rotation curve of the disc. In our case, $\Omega \propto r^{-3/2}$. In the computation of the Fourier decomposition of the perturbing function, the Laplace coefficient and its derivatives are involved;

$$b^m_{1/2} = \frac{2}{\pi}\int_0^{2\pi} \frac{\cos m\theta\, \mathrm{d}\theta}{\sqrt{1 - 2\alpha\cos\theta + \alpha^2}}. \tag{14}$$

As it is established in the literature, their computation is well approximated by means of the modified Bessel functions (K_ν). The integral may be approximated by $K_0(x)/\alpha^{1/2}$ (GT80), because now we cannot suppose $\alpha = 1$. In this approximation the coefficients are given by

$$b^m_{1/2} = \frac{2}{\pi}\frac{K_0(x)}{\alpha^{1/2}} \tag{15}$$

$$\alpha\frac{\mathrm{d}b^m_{1/2}}{\mathrm{d}\alpha} = \frac{-b^m_{1/2}}{2} - \epsilon m\left[\frac{\alpha+1}{\alpha}\right]K_1(x) \tag{16}$$

$$\alpha^2\frac{\mathrm{d}^2 b^m_{1/2}}{\mathrm{d}\alpha^2} = -\alpha\frac{\mathrm{d}b^m_{1/2}}{\mathrm{d}\alpha} + \frac{1}{\pi}\left\{\frac{1}{2\alpha^{3/2}}\left[m^2\frac{(\alpha+1)^2}{\alpha} + 1\right]K_0(x) + \frac{\epsilon m}{\alpha^2}\left[\frac{(\alpha+1)^2 - 2}{\alpha - 1}\right] \quad K_1(x)\right\}, \tag{17}$$

with $x = m|1 - \alpha|/\alpha^{1/2}$.

For the potentials with $l = m$ we have the Lindblad 'circular' torque. Its effect on the perturber is an orbital decay. For the potentials $l - m = -\epsilon$ we have Lindblad 'eccentric' torque (calculated on those non-coorbital resonances), it is also negative on the planet.

For the potentials $l - m = -\epsilon$ (in the non coorbital case), the corotation torque depends of the vorticity gradient Σ/B, and in our case it produces an outward migration.

Although we know that in our simulations the most important effect is the Lindblad circular torque, we have decided, for reasons of completitude, to compute the contribution of each kind of torque. In the coorbital region, whose width is related with the zone of horseshoe orbits, the contribution to the torque was studied by Quinn & Goodman (1986), Ward (1991, 1992) and Wahde & Donner (1996). We will use the expression found by Ward (1992) because it is closely related with the linear theory described above:

$$T = 4\Sigma|A|Bw^4\frac{\mathrm{d}\,ln}{\mathrm{d}\,ln\,r}(\Sigma/B) \tag{18}$$

where A and B are the Oort constants and w is the radius of the coorbital region. For a sufficiently massive perturber (tidal radius greater than the height scale of the disc), $w \simeq R_{\rm H}$ (Quinn & Goodman 1986; Ward 1992). In our simulations, the fraction of particles with $z < R_{\rm H}$ is 0.9 for Jupiter, whereas for the one core mass planet it is 0.8, so we will adopt this approximation for the coorbital radius. With these assumptions equation (18) may be written as

$$T = \frac{9}{8}\Sigma\Omega^2 R^4_{\rm H}. \tag{19}$$

The migration from this term will be outwards.

Those planetesimals coorbiting with the perturber are the most susceptible to saturate resonances, because they are set into libration. We think that coorbital torque is not present, due to the strong perturbation of the disc in the cases of Jupiter and Saturn, and due to the saturation in the $M_{\rm c}$ case, because its speed of migration is not sufficient to drift across the coorbital zone in a time shorter than the time-scale of saturation. Nevertheless, the inclusion of this kind of torque makes a negligible contribution to the net one.

7 ANALYTICAL PREDICTIONS

To compute the resonant torque by analytical means, one of the most important questions to be analysed is the maximum m which is valid to include, to sum the contributions of the different sources of resonant torque. The preceding formulae were obtained

Table 4. Maximum m and the predicted torque by the 2D theory.

	m_{max}	Γ [$M_\odot$ au^2 yr^{-2}]
Jupiter	5	-120.1×10^{-9}
Saturn	6	-13.6×10^{-9}
Core	10	-0.37×10^{-9}

Table 5. *O*/*C* relationship between the observed torque, the one predicted by the resonant 2D theory and by the ejection of planetesimals.

O/*C*	Resonant	Ejection
Jupiter	0.01	0.81
Saturn	0.04	1.14
Core	0.38	7.85

neglecting azimuthal gradients of quantities describing the flux in the neighbourhood of the resonances. Therefore, the torque increases without limits in the region surrounding the planet. On the other hand, one of the implicit assumptions of the theory is that no overlapping of resonances should occur. The theory ceases to be valid in this region.

The resonance-overlapping criterion (Chirikov 1979) gives a way to compute the m_{max} as (Wisdom 1980)

$$\frac{1}{m_{max}-1} \leq 2.1\mu^{2/7}, \tag{20}$$

where $\mu = M/M_\oplus$.

The m obtained in this way is not necessarily related to the actual last active resonance. Nevertheless, we don't want numerical proof of the theory, but to see how the theory represents the results of our simulations.

In Table 4 the m_{max} and the net torque (including those components coming from the Lindblad circular and eccentric resonances, the corotation resonances and the indirect part of the perturbing function) for the three cases are given. The coorbital torque has not been included for the reasons cited above.

The most important contribution comes from the Lindblad circular torque as is expected from the planetary eccentricities, and from the relevant wave numbers. All quantities were evaluated at resonant (initial) locations and with the non-perturbed density. All the torque expressions were evaluated at the same m_{max}.

Then we calculated the relation between the 'observed' torque (Table 2), and the 'calculated' one (Table 4). The *O*/*C* relation is 0.01 for Jupiter, 0.04 for Saturn and 0.38 for M_c. They are shown in the Table 5. These kind of estimates, similar to the ones given in works on gaseous discs, enable us to compare the distribution of the migration velocity in our simulations with the theoretical distribution given by Ward (1997). Type I migrators are defined as the planets which follow the predictions of the linear theory, and their velocities of migration are proportional to the planetary mass (the characteristic time-scales are inversely proportional to the mass). Type II migrators are in a non-linear regime. In this case the planet clears a gap and the orbital evolution becomes independent of the planet mass. In this case the orbital evolution can be orders of magnitude less than in type I. Extrapolating this result to our simulations, we should conclude that the discrepancy between the prediction of the 2D linear theory and the torque observed in the numerical simulations is due to non-linear effects, which introduce a strong disc profile modification. In Fig. 7 we show the 'dynamical heating' of the disc by a M_c planet. In planetesimals discs, this phenomena produces scattering (Ida & Makino 1993), and ejection.

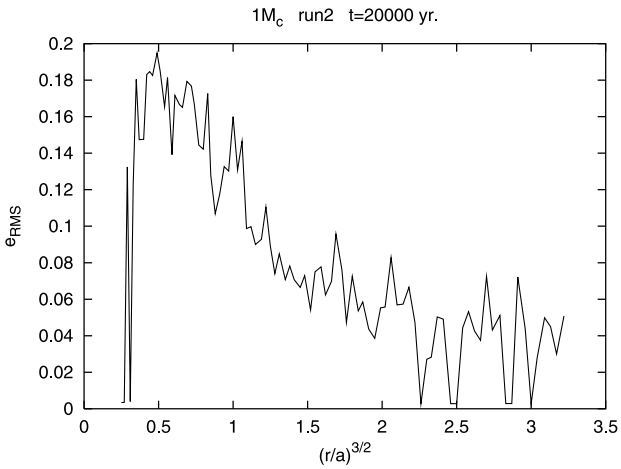

Figure 7. Rms eccentricity of the disc in one of the M_c simulations at $t = 20\,000$ yr averaged over bins of width 0.1 au.

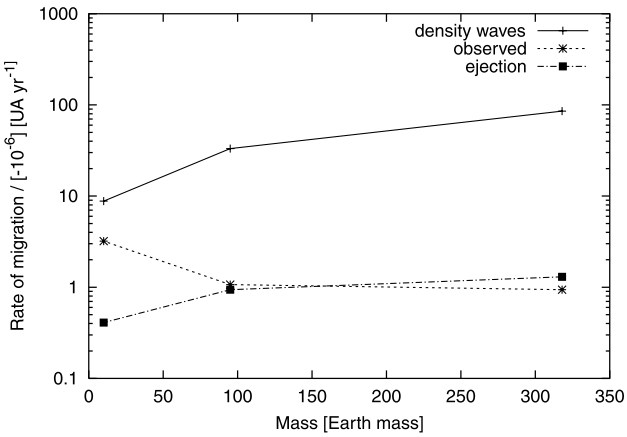

Figure 8. Migration rate calculated by 2D density waves theory (solid line), the 'observed' in our simulations (dashed line) and the result from the ejection(dash-dotted lines).

The effect of the ejection of particles may be evaluated by means of equation (2). We found that the torque due to ejection (for each case, averaged from the ejection of the four runs during the corresponding time interval) is 0.81 times the one observed in the case of Jupiter, 1.14 for Saturn and 7.85 for M_c. In Fig. 8 we show the relation between the observed torque and the calculated ones. The *O*/*C* relationship for both types of theoretical estimation are shown in Table 5. Although these estimations are very crude, they suggest, together with the reduction predicted by the density waves theory, that in a planetesimal disc of minimum mass, planets with masses larger than M_c follow a law of transfer of angular momentum similar to type II migrators in gaseous disc. Taking into account the dispersion between the four runs, which may be attributed to the limitations of our numerical experiments as well as in the way the 'observed migration' was obtained, our results suggest that for values of the mass near M_c there is a transition zone between type II and type I migrators. This feature will be investigated in a forthcoming paper.

Table 6. Speeds of migration (in units of 10^{-6}) obtained from Ward (1986) (W), Ida et al. (2000) (Iet), and the numerical results of this paper (NS).

	$\langle e_{\rm rms}\rangle$	W	Iet	NS
Jupiter	0.20	23.83	8.94	0.94
Saturn	0.15	12.71	6.34	1.07
Core	0.09	3.53	3.02	3.22

For a quantitative comparison with gaseous discs, we have included the analytical prediction for type I migrator, by Ward (1986, their equation 34). It contains the 'cut-off' function (the diminution of the torque due to gaseous pressure effects), and was derived in a linear regime. It also contains the speed of sound, related to the dispersion of velocities $\sigma \simeq e_{\rm rms} V_{\rm K}$ for particled discs, where $e_{\rm rms}$ is the rms eccentricity of the disc particles, and $V_{\rm K}$ is its Keplerian velocity. We have also included a comparison using the equation (23) by Ida et al. (2000) for particled discs by close and distant encounters. It also depends on σ trough the eccentricity of the planetesimals.

Both formulations are sensitive to the dispersion of velocity; Ward's (1986) torque formula depends on σ^{-2}, and in Ida et al. (2000) the dependence is approximately σ^{-3}. These formulations show how the enlargement of σ (the dynamical heating) reduce the net torque. They show that the type I behaviour depends linearly on the perturber mass.

Table 6 shows the calculated values of the speed of migration using the formulae cited above, and $e_{\rm rms}$ averaged over the disc for each case. These velocities are larger than those obtained by simulations. However, the Ida et al. (2000) expression is closer to the numerical results due to its dependence on the velocity of dispersion. We also think that this formulation performs a more realistic treatment of the problem, as encounters are taken into account. Our calculated speed of migration by density wave is larger with respect to the Ward estimates (see Fig. 8). It is due to the non-inclusion of the gaseous 'cut-off' function.

Jupiter and Saturn are far from the regime of applicability of this formula; the strong dynamical heating dominates the migration by means of ejections. As we have already seen, they follow a distinctive regime of migration which is not mass-dependent. For $M_{\rm c}$ the agreement is remarkable, but if we use a $e_{\rm rms}$ closer to the gap zone (where the torque is strongest), the estimates fall under the numerical values in a factor of almost 3, so this case, we think, supports the reliability of the numerical simulations, but neither is enough for a definitive classification of this planet.

Then we hope that, in a gradual fashion, masses smaller than $M_{\rm c}$ follow the linear theory more and more closely.

8 CONCLUSIONS

We have performed *N*-body numerical simulations of the exchange of angular momentum between a massive planet and a 3D Keplerian disc of planetesimals. Our interest was directed to the study of the orbital migration of the planets an to the validity of the classical analytical expressions of the lineal theory of density waves in 2D, as representative of dynamical friction in discs 'dominated by the planet'. By means of a numerical integration of the equations of motion, we have carried out a set of numerical experiments with large number of particles ($N \geq 10\,000$), and planets of different masses between the mass of Jupiter and the mass of one core mass of the giant planets in the Solar system ($M_C = 10\,{\rm M}_\oplus$).

We studied the semi-major axis evolution and determined a zone to measure the torque on the planet. The main conclusions are as follows.

(i) The net migration is always inwards in a disc of small density ($\sim 10\,{\rm g\,cm^{-2}}$), compatible with a minimum mass solar nebula model. The time-scale of orbital decay is of $\sim 10^6$ yr for all the cases under study.

(ii) The rate of migration in a minimum mass solar nebula, due to the solid phase, does not enhance the accretion rate on the planet in a time-scale relevant for giant planet formation.

(iii) We have estimated the resonant component of the torque and we have computed the relation between the 'observed' torque (Table 2), and the 'calculated' one (Table 4). The *O*/*C* relation is 0.01 for Jupiter, 0.04 for Saturn and 0.38 for $M_{\rm c}$.

(iv) The dynamical heating of the disc is responsible for the reduction of the net resonant torque on the planet. Therefore, in addition to the fact that the migration rates are almost the same for the biggest planets we conclude that this planets evolves as following the definitions of the types II migrators in gaseous discs. Taking into account the reduction of the resonant torque for $M_{\rm c}$, planets with masses smaller than it would be well described by the linear theory of density waves in a planetesimal disc compatible with the minimum-mass solar nebula.

We cannot say anything with respect to the final destiny of the planets. As a result of the time-span of the simulations, they fail to explain any switch-off of this mechanism of migration, which must be related to the involved time of relaxation, even thought it must be orders of magnitude larger.

Finally, for a complete comparison of migrators in planetesimal and gaseous discs, a more wide range of planetary masses should be simulated (the smaller ones), in particular, for the study of the transition stage between the two types of orbital evolution. We think, in accordance with Ida & Makino (1993), that at 5 au this stage appears between $0.1\,{\rm M}_\oplus$ and masses smaller than $M_{\rm c}$.

ACKNOWLEDGMENTS

We thank the anonymous referee for useful suggestions that improved the presentation of our work. RGC is very grateful to UTN - Facultad Regional San Nicolás (FRSN) for its hospitality, specially Ing. Neoren Franco, Dr. Roberto Caligaris and Lic. Georgina Rodriguez. The computational resources of the Centro de Estudios y Desarrollos Informaticos (CEDI) of the FRSN are gratefully acknowledged.

REFERENCES

Artymowicz P., 1993, ApJ, 419, 166
Chambers J. E., 1999, MNRAS, 304, 793
Chandrasekhar S., 1942, Principles of stellar dynamics. The Univ. of Chicago Press, Chicago, Illinois
Chirikov B. V., 1979, Phys. Rep., 52, 263
Danby J. M. A., 1962, Fundamentals of Celestial Mechanics. Willmann-Bell Inc., Richmond, Virginia
Fernández J., Ip W., 1984, Icarus, 58, 109
Goldreich P., Tremaine S., 1979, ApJ, 233, 857 (GT79)
Goldreich P., Tremaine S., 1980, ApJ, 241, 425 (GT80)
Ida S., 1990, Icarus, 88, 129
Ida S., Makino J., 1992, Icarus, 98, 28
Ida S., Makino J., 1993, Icarus, 106, 210

Ida S., Bryden G., Lin D., Tanaka H., 2000, ApJ, 534, 428
Kley W., D'Angelo G., Henning T., 2001, ApJ, 547, 457
Landau L. D., Lifshitz E. M., 1959, Fluid Mechanics. Pergammon Press, London
Lissauer J., 1993, ARA&A, 31, 129
Lynden-Bell D., Kalnajs A. J., 1972, MNRAS, 157, 1
Miyoshi K., Takeuchi T., Tanaka H., Ida S., 1999, ApJ, 516, 451
Murray N., Hansen B., Holman M., Tremaine S., 1998, Sci, 279, 69
Nelson R., Papaloizou J., Masset F., Kley W., 2000, MNRAS, 318, 18
Pollack J. B., Hubickyj O., Bodenheimer P., Lissauer J. J., Podolak M., Greenzweig Y., 1996, Icarus, 124, 62
Quinn P. J., Goodman J., 1986, ApJ, 309, 472
Safronov V. S., 1972, Evolution of the Protoplanetary Cloud and the Formation of the Earth and the Planets. Nauka Press, Moscow
Takeda H., Matsuda T., Sawada S., Hayashi C., 1985, Prog. Theor. Phys., 74, 272
Tanaka H., Ida S., 1999, Icarus, 139, 350
Tanaka H., Takeuchi T., Ward W. R., 2000, Lunar and Planetary Science, 31, 1418
Wahde M., Donner K. J., 1996, A&A, 312, 431
Wahde M., Donner K. J., Sundelius B., 1996, MNRAS, 281, 1165
Ward W., 1986, Icarus, 67, 164
Ward W. R., 1988, Icarus, 73, 330
Ward W. R., 1991, Lunar and Planetary Science, 22, 1463
Ward W. R., 1992, Lunar and Planetary Science, 23, 1491
Ward W. R., 1997, Icarus, 126, 261
Ward W. R., Hahn J. M., 1995, ApJ, 440, L25
Wisdom J., 1980, AJ, 85, 1122
Wisdom J., Holman M., 1992, AJ, 102, 1528

This paper has been typeset from a TEX/LATEX file prepared by the author.